CHEMMEDCHEM

DOI: 10.1002/cmdc.200900320

Structural Model for the Binding Sites of Allosterically Potentiating Ligands on Nicotinic Acetylcholine Receptors

Edgar Luttmann,[a] Jürgen Ludwig,[b] Anja Höffle-Maas,[b] Marek Samochocki,[b] Alfred Maelicke,[b] and Gregor Fels*[a]

Current treatments of Alzheimer's disease include the allosteric potentiation of nicotinic acetylcholine receptor (nAChR) response. The location of the binding site for allosteric potentiating ligands (APLs) within the receptor is not yet fully understood. Based on homology models for the ligand binding domain of human α7, human $\alpha4\beta2$, and chicken α7 receptors, as well as blind docking experiments with galanthamine, physostigmine, codeine, and 5HT, we identified T197 as an essential element of the APL binding site at the outer surface of the ligand binding domain (LBD) of nAChR. We also found the previously known galanthamine binding site in the region of K123 at the inside of the receptor funnel, which, however, was shown to not be part of the APL site. Our results are verified by site-directed mutagenesis and electrophysiological experiments, and suggest that APL and ACh bind to different sites on nicotinic receptors and that allosteric potentiation may arise from a direct interplay between both these sites.

Introduction

Nicotinic acetylcholine receptors (nAChRs) are believed to play a key role in Alzheimer's disease (AD), a neurodegenerative disease strongly linked to the failure of synaptic transmission. AD is accompanied by a loss of neurons, the appearance of characteristic protein aggregates,[1,2] and a severe loss of nicotinic receptors.[3–5] Most successful anti-dementive drugs in current use are based on the inhibition of acetylcholinesterase (AChE), resulting in increased levels of acetylcholine (ACh).[6–8] This results in increased stimulation of nAChRs.[9,10] The alkaloid galanthamine, in addition to being a moderate AChE inhibitor, acts as an allosteric potentiating ligand (APL) on the nAChR, thereby enhancing the response to agonist stimulation of the receptor.[11–16] Other compounds acting as APLs are the AChE inhibitor physostigmine, the morphine derivative codeine, and the neurotransmitter 5-hydroxytryptamine (5HT).[11–13,17–20] This is supported by experimental evidence from ligand binding studies with the APLs,[13,17] electrophysiological measurements on cell lines and primary cultured neurons,[13] and by competition studies with the antibody FK1,[11,21] which selectively modulates APL binding. Of particular importance for the study reported herein is the property of the monoclonal antibody FK1 to selectively block the APL binding site without affecting the ACh binding site.

The mode of action by which galanthamine and other APLs enhance the sensitivity of nicotinic receptors to agonists is not yet fully understood. There is evidence that APLs enhance the probability of agonist-mediated channel opening,[22] stabilize the open-channel state of nicotinic receptors, enhance agonist-induced responses,[16,20] and decrease or overcome desensitization of nicotinic receptors.[23] That the APL binding site is separate from the ACh binding site has originally been suggested by photoaffinity labeling experiments with [^{3}H]physostigmine, which selectively labels lysine 125 of the *Torpedo* sp. nAChR.[24] The sparse experimental knowledge about the APL effect motivated us to use homology modeling and molecular docking to learn more about the structural basis of the allosteric effect. This became possible with the publication of the crystal structure of an acetylcholine binding protein (AChBP) found in the snail *Lymnaea stagnalis*,[25] and from *Aplysia californica*[26] a non-channel homolog of the extracellular domain of nAChRs. Further structural knowledge is available from recently published crystal structures[25,27–33] and electron microscopy studies by Unwin and co-workers.[34–37] AChBP shares ~25% sequence identity with nAChR and has the same pentameric assembly and high homology to the ligand binding domain (LBD) of nAChRs. Several models of the nAChRs or parts of this transmembrane protein have been published.[36,38–49]

Herein we present models for the extracellular portion of the chicken α7, the human α7, and the human $\alpha4\beta2$ nAChR extracellular domains. All models were used in ligand docking with ACh, nicotine, and epibatidine to evaluate the models by comparison with experimental results. Subsequently, the models were used to identify possible binding sites for APLs by searching for cavities and blind docking experiments with several APLs. Our studies originally predicted five potential APL

[a] *Dr. E. Luttmann, Prof. Dr. G. Fels*
University of Paderborn, Department of Chemistry, Warburger Straße 100, 33098 Paderborn (Germany)
Fax: (+49) 5251-60-3245
E-mail: fels@uni-paderborn.de

[b] *Dr. J. Ludwig, Dr. A. Höffle-Maas, Dr. M. Samochocki, Prof. Dr. A. Maelicke*
Current address: Galantos Pharma GmbH, Biotechnikum an der Goldgrube, Freiligrathstraße 12, 55131 Mainz (Germany)

Supporting information for this article is available on the WWW under http://dx.doi.org/10.1002/cmdc.200900320.

sites, one of which is equivalent to the ACh binding site of AChBP that has recently been shown in co-crystallization experiments with *Aplysia* sp. AChBP to bind galanthamine as well.[26] More importantly, however, two of our putative APL binding regions are in agreement with experimental data connected to the allosteric effect exhibited by galanthamine.[21] One of these is located at the outer surface in the vicinity of, but not identical to the ACh binding site, and the other is found in the vicinity of lysine 125 (*Torpedo* sp. numbering), which has previously been identified as part of the APL site by radiolabeling experiments with physostigmine.[24]

Based on these results, we performed site-directed mutagenesis studies of ectopically expressed chimeric chicken α7/mouse $5HT_3$ receptor channel complex, in combination with whole-cell current measurements, in the presence and absence of the prototypic APL galanthamine.[50] We demonstrate that T197 and, to a smaller extent, I196 and F198 are involved in APL binding at the outer surface of the receptor funnel, whereas K123 (the corresponding residue to K125 of *Torpedo* sp.) is not part of this site, but rather represents a binding site from which galanthamine might exert its noncompetitive inhibition.[15] Our computational data further confirm that APLs bind to a site on nicotinic receptors that is separate from the ACh binding site, but close enough to enable synergistic activation of the receptor channel.

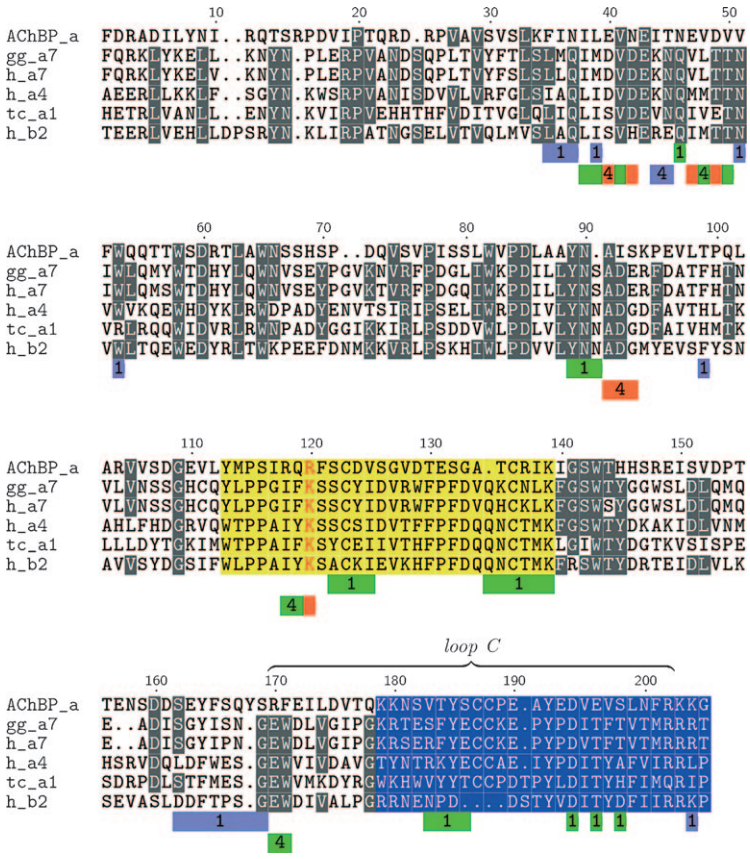

Figure 1. Multiple sequence alignment for the sequences involved in the nAChR subtypes used in this study. Loop C is indicated for orientation, and the experimentally known features are highlighted as follows: The radiolabeled K123 (K125 in *Torpedo* sp. numbering) is shown in red text. Protein stretches with high and medium affinities for antibody FK1 binding are shown in yellow and blue, respectively. The two identified putative APL binding sites are marked with the bars labeled 1 and 4, with the clockwise face of the binding pocket colored in green and the counterclockwise face in cyan. For the APL binding site 4, residues in dark cyan indicate their simultaneous contribution from both faces. Subunit specification: AChBP_a = AChBP α, gg_a7 = chicken α7, h_a7 = human α7, h_a4 = human α4, tc_a1 = *Torpedo californica* α1, h_b2 = *human* β2.

Results and Discussion

Structure of the ligand binding domain

The multiple sequence alignment used in this study is depicted in Figure 1. This alignment was calculated with CLUSTAL-X on the basis of the AChBP–carbamylcholine complex[29] and manually refined to match the alignment from Le Novere et al.,[38] resulting in sequence identities ranging from 20 to 50%. The experimentally determined features are marked along the sequence (Figure 1). Two features are particularly relevant to our investigation: 1) K123 (K125 in *Torpedo* sp. numbering; red text in Figure 1), which in a photoaffinity labeling study with the APL physostigmine was shown to carry the radioactive label,[24] and 2) the protein stretches that show high (highlighted in yellow) and medium (highlighted in blue) affinities for the monoclonal antibody FK1, which selectively blocks the APL binding site.[11,21] Figure 1 also depicts the two putative APL binding sites that are the results of this study. Of these two putative APL sites the bars numbered 1 represent the outer binding site around T197, whereas those numbered 4 depict the region inside the funnel in the vicinity of K123.

The overall three-dimensional structure of the LBD is very similar in all the models, as the models were based on the same AChBP template (PDB code: 1UV6, carbamylcholine in complex with AChBP).[29] Figure 2 shows the gross features of the models: the composition of five subunits, the central pore, and the relative locations of the ligand binding site located underneath the adjacent cysteine-containing loop C (shown in black).

Ligand binding site

As a preliminary check of the procedure employed, we docked known ligands (ACh, nicotine, and epibatidine) in a blind docking experiment and verified that the ligands bind preferentially to the correct binding site. The wealth of experimental data and recent crystal structure solutions of the AChBP–carbamylcholine complex[29] allow comparison with the docking data, which show very similar results, as depicted in Figure 3.

Blind docking of ACh in any of the various models exclusively resulted in docking solutions inside the ligand binding sites underneath loop C. All ligand binding sites are populated, and only two main orientations of ACh are found. In these two

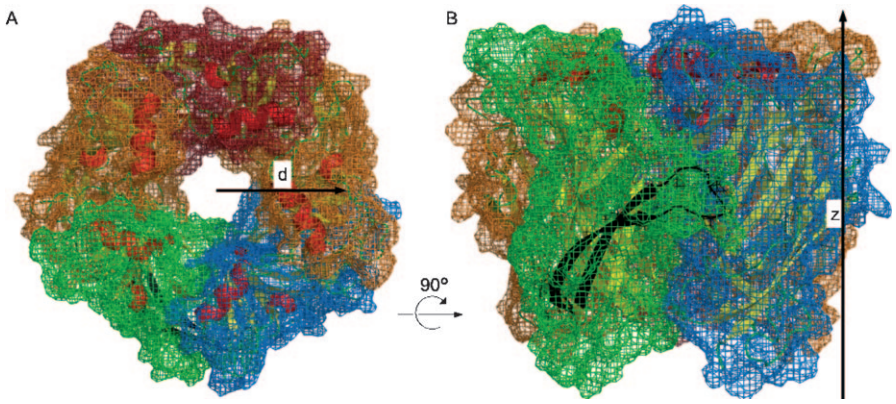

Figure 2. Model of the ligand binding domain (LBD) from the chicken α7 homopentamer, with each subunit given in a different color. A) The top view displays the fivefold pseudo-symmetry of the receptor and the central pore where the ions pass. B) The side view, as seen from the outside, indicates the contact surface between two subunits and the loop C double-Cys finger (black loop) extending from the (+) subunit (green) over to the neighboring (−) subunit (cyan). The tip of the loop C covers the agonist binding site (indicated by the black box). For orientation, two geometric parameters are indicated: *d* for the distance from the central pore axis and *z* along the pore axis with the origin being in the center of the LBD.

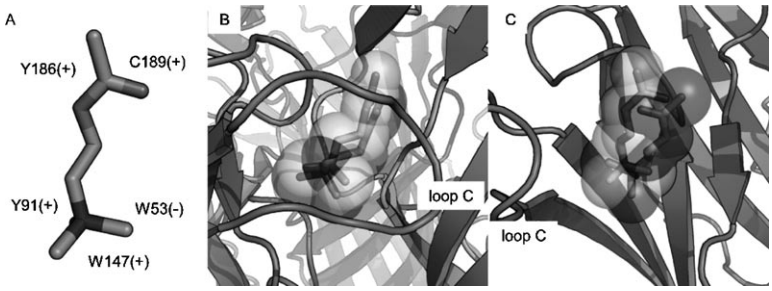

Figure 3. Best ACh binding mode from the chicken α7 receptor: A) schematic view, B) overlaid with the carbamylcholine from the X-ray crystal structure viewed from the outside through loop C, and C) in the (+) face of the contact surface. The schematic view indicates the interacting residues for this binding mode, with all contacts being hydrophobic. The two ribbon representations show the carbamylcholine X-ray crystal structure solution and the best ACh docking mode with superposition of the quaternary nitrogen atoms; notable are the highly similar occupied volumes (color image available in the Supporting Information).

binding modes the quaternary nitrogen atom is positioned in identical locations and only the tail of the molecule is directed toward (−*z*) or away from (+*z*) the cell membrane. Figure 3 depicts the most favorable binding mode from the ACh docking experiments with the gg_a7 receptor (chicken α7), with the acetyl tail of the molecule pointing upward (+*z* direction, or away from the cell membrane). All interacting residues were previously found in experimental studies to be part of the ligand binding site (e.g., radiolabeling and mutational studies as reviewed by Arias[51]). Overlaying the best docking pose with the carbamylcholine from the corresponding AChBP crystal structure[29] shows the superposition of the charged nitrogen atom. The acetyl and carbamyl tails of the two different molecules point in a similar direction, but they diverge slightly, as is apparent from the side view (Figure 3C). Docking with nicotine and epibatidine (data not shown) is in similar agreement with experimental evidence. This indicates that the employed scoring function of FlexX is capable of identifying poses similar to the crystal structure; that is, it demonstrates the capability of FlexX to reproduce known experimental findings. One should, however, keep in mind that a putative APL site could be located in an area different from the ligand binding site and that a correct positioning of carbamylcholine, nicotine, and epibatidine does not necessarily prove a correct finding in a blind docking experiment with APL.

Putative APL binding sites of the nAChRs

In the search for the APL binding site, we used alpha spheres, a special tool in MOE[52] that helps locate potential ligand binding sites (cavities), which are a generalization of convex hulls developed by Edelsbrunner and colleagues.[53] We also used blind docking methods to identify the location and orientation of ligands as an unbiased procedure of finding docking solutions anywhere on the protein without restricting the search to certain areas of the target. This methods has also been used by Iorga et al.[40] to locate potential binding sites for physostigmine, galanthamine, and codeine on human α7, α4β2, and α3β4 receptors.

The localization of cavities with alpha spheres is shown in Figure 4 which identifies five major cavities (filled with the gray alpha spheres). These are the ligand binding site for agonists/antagonists underneath loop C (2) (see also Figure 3) and two further cavities on the outside of the receptor, one at the lower (1) and one at the upper (3) entrance to the ligand binding site. In addition, there are two cavities on the inside of the receptor, lining the pore (Figure 4B). The inner binding sites are located at both sides of a bulge, separating them into a lower (4) and an upper (5) inner cavity.

These results are very similar in all the examined models and thus, we only report herein the results for the LBD of the chicken α7 receptor. Throughout this paper we present the computational data on chicken α7, because probing of APL binding by analysis of selected mutations, as described below, was done with chicken α7/5HT$_3$ nAChR.[50] Additional results on human α7 and α4β2 are given in the Supporting Information (figures S1 and S2).

Results from blind docking experiments with the four APL ligands galanthamine, physostigmine, codeine, and 5HT (Figure 5) are depicted in Figure 6. As can be seen, there are

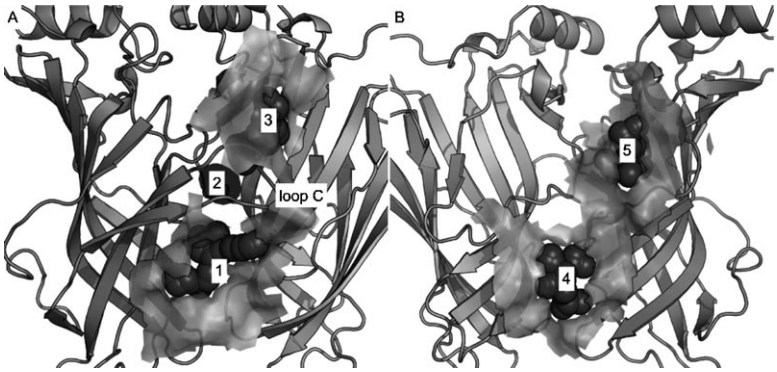

Figure 4. Alpha spheres within a dimer of the LBD. A) There are three principal cavities (1–3) on the outer surface of the LBD: below loop C (1), covered by loop C (2), and above loop C (3). All cavities are formed at the dimer interface. The contributions from the two monomers can be seen in the color image in the Supporting Information. B) The inner surface of the LBD shows two major cavities, one at the lower part (4) and a second one located closer to the cytoplasm (5).

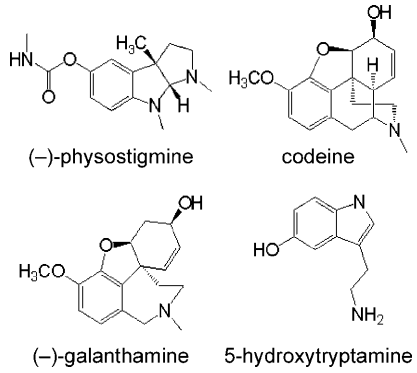

Figure 5. Structures of APL used in blind docking experiments with the receptor models.

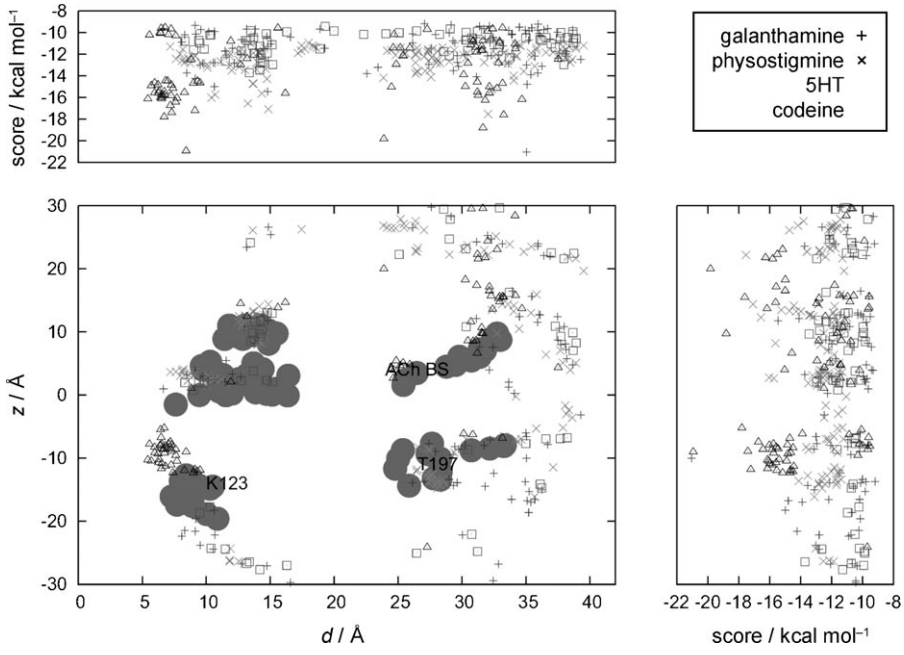

Figure 6. Docking results projected into the distance (*d*) and leverage (*z*) plane of the chicken α7 LBD (see the Supporting Information for a color image and for analogous figures for human α4β2 and human α7 heteropentameric LBDs). Each binding mode for the ligands employed is marked at its center of mass position. The two lining graphs indicate the score for each docking pose. The filled circles indicate the alpha spheres and thus putative binding sites. The center of the ACh binding site (ACh BS) and Cα of K123 are marked for orientation.

many more potential binding sites found by docking than those extracted by the alpha sphere technique, which underscores the difference between the two methods. While alpha spheres only depict cavities at the protein surface, docking techniques find the ligand anywhere on the surface where a reasonable attractive interaction between protein and ligand occurs. The central plot of Figure 6 shows, for each cluster representative, the distance (of the center of mass) from the central pore axis (*d*) and the position along the pore axis (*z*) relative to the LBD center (schematically shown in Figure 2). In addition, the plots show the average docking score for each cluster as a function of the same geometrical parameters. The computational output is very noisy, and docking results are observed in many locations on the surface of the protein. However, several areas on the surface show a clustering of docking results and thus indicate putative binding sites.

Figure 6 also indicates the positions of the alpha spheres in the same reference frame, thus permitting identification of binding modes inside the cavities found. The clustering of the alpha spheres overlaid with the docking modes suggests several putative binding pockets, with better resolution to the alpha sphere analysis alone. From Figure 6 it is possible to distinguish more than just five pockets. For example, the inner upper (small *d*, $+z$) and outer lower binding site (large *d*, $-z$) can be split into smaller clusters. For this study we do not use this finer resolution, and thus the above-described classification into five cavities is used. A unique binding pocket for the APLs cannot be identified, as all cavities contain docking solutions or have some in close vicinity. The docking scores are also unable to distinguish between the binding sites. Neither the inside nor the outside (see upper energy plot in Figure 6) and neither the upper nor the lower binding site (see right energy plot in Figure 6) show favored binding.

Consensus construction

In an attempt to evaluate the docking results in view of the five alpha spheres as potential binding sites, we related the results to experimental data. Residue K123 (corresponding to K125 of the *Torpedo* sp. nAChR α subunit), which was identified previously by radiolabeling experiments with physostigmine[24] as part of the APL site, is located in close proximity to the lower inner binding site (4 in Figure 7). Therefore this area

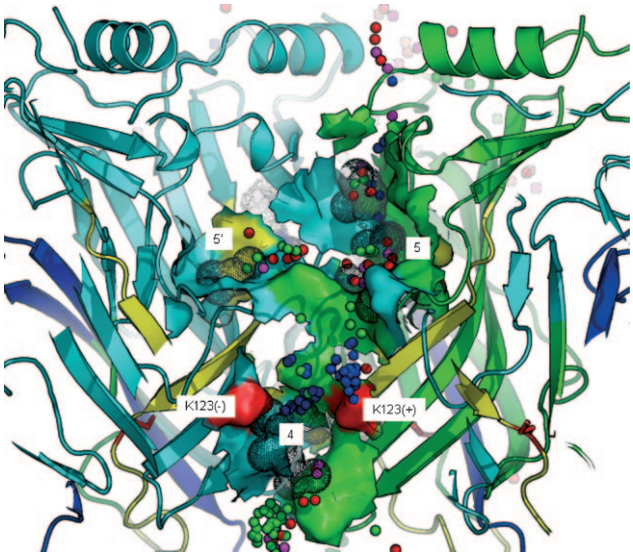

Figure 7. View of the inner surface of the LBD. Two of the five protein chains are shown in cyan and green. The alpha spheres are indicated by the dark dotted spheres, and docking modes from the cluster analysis are given as small solid spheres at the geometric center of each cluster representative (galanthamine: red, physostigmine: green, codeine: purple, and 5HT: blue). K123 is depicted by the red surface patch, and the high- and medium-affinity protein fragments from the antibody FK1 binding experiments are given in yellow and blue, respectively.

should be a potential candidate for APL binding. Furthermore, protein fragments of the nAChRs that were identified with medium and high affinity to the FK1 antibody[21] (blue and yellow, respectively, in Figures 7 and 8) overlap strongly particularly with the lower outer binding site (Figure 8). In contrast, the alpha sphere that specifies the ligand binding site can be excluded, as the APL ligands investigated in the docking experiments are known to act noncompetitively with ACh and other agonists from separate, albeit neighboring, sites at the receptor surface.[20,22,50]

Closer examination of the LBD interior (Figure 7) identifies the following features at the lower inner binding site (4): a) a small cluster of alpha spheres indicates a cavity (black dotted spheres), b) K123 residues from two adjacent subunits are in close proximity (see the red surface patches), c) binding modes from all four APLs (small solid spheres) used in docking experiments are found close to this binding site, and d) the protein residues forming the pocket overlay partly with a fragment identified to bind FK1 (yellow strand).

Physostigmine shows a few docking modes (green solid spheres) neighboring the K123 residues (red surface patches).

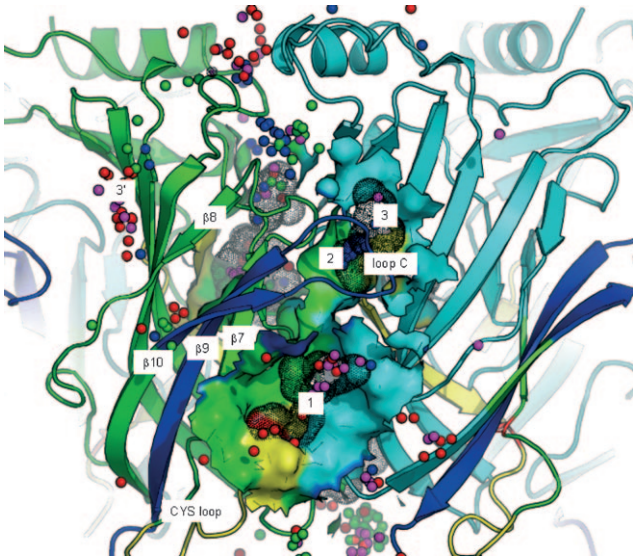

Figure 8. View onto the outer surface of the LBD. Coloring is the same as in Figure 7 with the surface of loop C removed to allow a view into the ligand binding site.

Photoaffinity labeling experiments with this ligand were indicative of K123 being an essential amino acid for APL binding;[24] Costa et al.[39] and Iorga et al.[40] have also described this region as the putative APL binding site.

Notably, due to its size relative to the receptor aperture, the antibody FK1 cannot reach into the pore. Thus FK1 cannot bind to an assembled receptor at the lower inner binding side of the LBD. However, the APL inhibitory effect of the FK1 antibody itself may be due to an allosteric effect, as antibody binding to the outside of the receptor may result in a conformational change transmitted through the protein to the inside of the LBD, altering the binding affinity of APLs. Schroeder et al. have shown that such a transmission appears to be unaffected, because the antibody competes with physostigmine.[21] As the mechanisms of channel gating and its allosteric modulation remain unknown, none of these modes of action can be ruled out.

Results of the modeling experiments combined with experimental data,[11,21] as summarized in Figure 8, favor the lower outer cavity (site 1) over the upper outer location as a potential APL binding site. This decision is particularly based on results from epitope mapping studies with the FK1 monoclonal antibody,[21] which acts as a selective macromolecular antagonist of the APL galanthamine without affecting basic activation of the receptor's integral cation channel by nicotine.[15,54,55] The lower outer cavity is located in an area that is confined by parts of β strands 7 and 10, which are known to show high- and medium-affinity binding to FK1, respectively. In contrast, the upper outer cavity (site 2), which is close to the upper entrance to the ligand binding site, is only flanked by parts of β strand 10. It is remarkable that the lower outer cavity particularly binds galanthamine, codeine, and 5HT, while the lower inner binding site also has massive docking solutions with physostigmine.

In conclusion, our results propose either the lower inner (1) or the lower outer binding site (4) as the APL binding site, but are unable to distinguish between these two sites. However, the findings allow a mapping of the two binding sites and thus a suggestion of a few targeted mutational experiments that should influence APL binding. The individual residues contributing to both binding sites are marked in Figure 1 by the bars underneath the alignment and are given in a tabular form in the Supporting Information (table S1). The contributions of the (+) and the (−) face are colored as before (green and cyan, respectively). Importantly, the putative APL binding site 4 contains identical residues from both faces (given in dark cyan in Figure 1).

Based on these results, we have selected the amino acids N92, K143, I196, T197, and F198 from the lower outer cavity, and P119, F122, and K123 from the inner cavity for mutation experiments. The complete experimental details and results are beyond the scope of this paper and are described in detail elsewhere.[50] In short, a series of chicken α7/mouse $5HT_3$ chimeric receptors was designed and transiently expressed in TRex-293 cells, with selected mutations of single-residue positions of the proposed APL binding regions, followed by whole-cell patch-clamp studies on the mutant receptors in the presence and absence of agonist and of the APL galanthamine (Figure 9).

From these experiments Figure 10 summarizes only the findings for the wild-type receptor (WT) in comparison with the two mutants (K123G and T197A). As shown in Figure 9, mutation of the charged polar and long lysine side chain to a nonpolar and short glycine side chain (K123G) neither affected activation of the mutant receptor by nicotine, nor did it affect potentiation of the agonist response by galanthamine. These experimental data suggest that K123 is neither an element of the APL binding site, nor is it essential for basic channel gating by agonist.

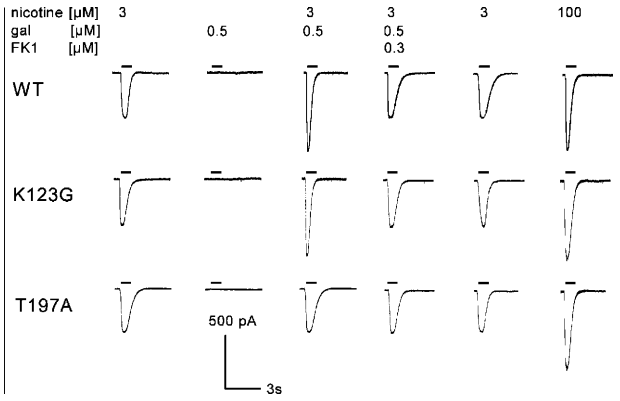

Figure 9. Electrophysiological measurements with wild-type (WT), K123G, and T197A mutant forms of the nAChR. The receptors where treated with 3 μM nicotine alone. After regeneration, addition of 0.5 μM galanthamine alone showed no effect. In the third experiment, nicotine and galanthamine were applied together and produce a stronger signal in the wild-type as well as in the K123G mutant. In contrast, the T197A mutant shows no effect after galanthamine binding, that is, the APL effect is completely abolished. The enhancement by gal of the response to nicotine was abolished in the presence of FK1 (fourth trace) and fully restored after washout (fifth trace). Moreover, enhancement by gal of K123G mutant whole-cell current was almost undistinguished from the maximal current (sixth trace) observed following nicotine stimulation. (Figure reproduced from Reference [50].)

Furthermore, mutation of the polar threonine to a nonpolar alanine (T197A) also did not affect basal agonist-induced activation of the chimeric receptor, indicating that this residue is not part of the agonist binding region of the receptor. However, in contrast to the mutation of K123, APL activity of galanthamine was completely abolished by mutation of T197, suggesting that T197 is indeed an essential element of the galanthamine binding site on nicotinic receptors. A similar but smaller effect was observed with I196G and F198L.[50]

Discussion

We have developed structural models for the extracellular region, the ligand binding domain (LBD) of chicken α7, human α7, and human α4β2 on the basis of published crystal structures of the acetylcholine binding protein from *Lymnaea stagnalis*.[29] The model was evaluated with respect to the ligand binding site by blind docking experiments with the nicotinic ligands acetylcholine, nicotine, and epibatidine as prototropic partners. Using the structural template of the LBD obtained in this way, blind docking experiments were performed with the APLs galanthamine, physostigmine, codeine, and 5HT, using all three receptor models. From these experiments two putative APL binding regions result which are separate from the agonist site,[21,24] and are in general agreement with the conclusion previously drawn from photoaffinity labeling studies with physostigmine,[24] and from epitope mapping studies with the FK1 monoclonal antibody.[21]

One region is located on the outside of the receptor, with T197 and, to a smaller extent, I196 and F198 as essential elements, a binding site that has previously not been described. The second site is located around K123, and is equivalent with the location previously identified by physostigmine labeling by Schrattenholz et al.[24] This site also resembles the binding regions previously described.[39,40] In those studies, Costa et al.[39] examined a putative APL binding site in great detail with physostigmine for α3β4 and α4β2 receptors. This work restricted the search to the surface area in the vicinity of the lysine residue previously identified by radiolabeling experiments as part of an APL binding site.[24] Furthermore, we also found the three binding sites described by Iorga et al.,[40] who used a blind docking approach similar to our procedure. They used physostigmine, galanthamine, and codeine as APL ligands on human α7, α4β2, and α3β4 receptors with a different docking algorithm (AutoDock[56]). The three identified binding sites agree well with the binding sites we found on the inner surface of the receptor, but they have not identified binding sites on the outside of the receptors.

Importantly, we also found galanthamine binding to the binding site for agonists/antagonists underneath loop C. This is in agreement with a recent study by Hansen and Taylor, who co-crystallized galanthamine with AChBP from *Aplysia* sp., and found galanthamine bound to four of the five identical agonist binding sites of this homopentamer.[26] This result is consistent with the extremely close sequence similarity of the agonist

binding region of chicken α7, human α7, and human α4β2 on the one hand, and the AChBP α subunit on the other hand. In contrast, however, the APL binding region for galanthamine around T197, as found in our studies, is quite different from the α subunits of AChBP, in which I196, T197, and F198 are absent but rather substituted by Val, Asn, and Leu, respectively. In addition, this surface region only resembles a very shallow trough in the *Aplysia* sp. AChBP α subunit, which would not be suitable for ligand binding.

Notably, we restricted our work to blind docking because a further investigation of individual interactions that contribute to the binding of a ligand by a refined docking procedure using modeled structures is an ambitious task; this is because: 1) the homology models are somewhat ambiguous in the orientation of their side chains, 2) the protein is kept fixed during our docking protocol, and 3) no induced fit of the protein was allowed. The only protein flexibility we account for stems from the redundant contact surfaces we used during docking. Thus we have five or two similar binding sites (for the homo- or the heteropentamers, respectively) with slightly varying side chain positions.

Electrophysiological studies with selected mutants of the $\alpha7/5HT_3$ chimeric receptor, however, strongly suggest that a binding site for allosterically potentiating ligands (APL) is formed at the outer surface of the nAChR LBD by participation of β strand 10 residues I196, T197, and F198, with T197 probably being an essential attachment point for this type of nicotinic ligand.[50] This site is part of the FK1 epitope and is probably the one from which cooperativity with agonist in channel opening[20] and weak noncompetitive agonism[22] are induced.

Residues I196, T197, and F198 are located in β strand 10, directly connected to D195, which together with Y186 and K143 has been proposed by Mukhtasimova et al.[57] to be responsible for a conformational change upon ACh binding, which in turn, could be responsible for channel opening (Figure 10). The putative APL binding site is situated in the vicinity of, but separate from, the ACh site, and as shown in Figure 10, should be accessible for the binding of large proteins such as antibody FK1. I196, T197, and F198, on β strand 10, are direct neighbors of K143 on β strand 7, which has been proposed by Criado et al.[58] as well as Ludwig et al.[50] to play a role in the coupling of agonist binding to channel opening and closing. In addition to being flanked by T197, K143 is juxtaposed on the other side by Asn 92, which was recently shown to be the major connection point for bungarotoxin, which blocks ligand binding and consequently APL effects.[30] The location of K143 between the ACh site and the Cys loop suggests that upon APL binding, a conformational change is induced that enhances the affinity for agonist binding and/or leads to an improved coupling of the agonist binding region to the channel gating region. The identified site clearly differs from that previously proposed by Schrattenholz et al.[24] and Iorga et al.[40]

The question as to whether there is a second binding site for APL ligands located at the inner side of the channel might be answered as follows: Electrophysiological studies have indicated that there are indeed at least two types of binding site for galanthamine and compounds with similar function.[15,55]

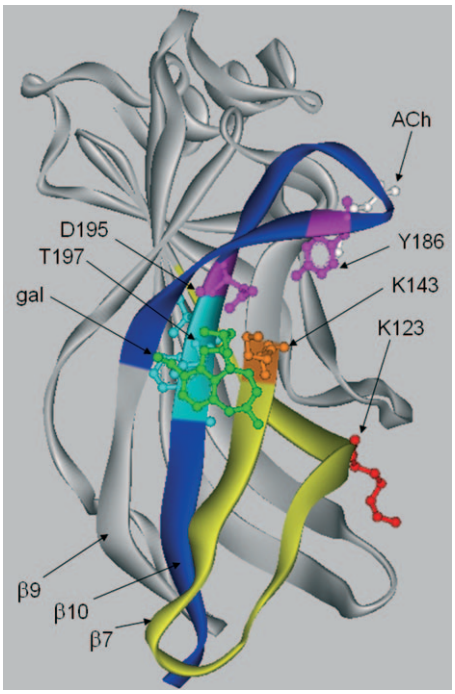

Figure 10. Ligand binding domain (LBD) of a single α subunit of chicken α7–nAChR. Galanthamine (gal, green) is shown in a typical position in the lower outer binding site characterized mainly by I196, T197, and F198 (turquoise). Additionally, K143 (brown), which has been proposed to be involved in binding–response coupling,[50] has also been proposed, together with Y186 and D195, to trigger channel opening on ACh (white) binding.[57] For comparison, K123, which was previously shown to be labeled by [^{14}C]physostigmine, is also shown (red).[24] High- and medium-affinity protein fragments from the antibody FK1 binding experiments are given in yellow and blue, respectively.

One of these is the APL site, which is of higher affinity and which is responsible for facilitating the agonist-induced channel opening, as shown in Figure 9. The second is the binding site for noncompetitive inhibitors (NCI), which is of lower affinity and which affects the receptor by channel blocking. Experimental evidence from epitope mapping experiments with monoclonal antibodies (mAb) indicates that this second site could be located at the inner surface of the receptor funnel.[21,59] Experiments using mAb FK1, which selectively blocks the APL binding site, and mAb WF6, which selectively blocks the agonist binding site, together with photoaffinity labeling using radioactive physostigmine[24] have made clear that the binding sites on nicotinic receptors for agonist and for APL are separate but neighboring entities.[21,24,59] In addition, it was suggested that Lys 125 of the α subunit extracellular domain of *Torpedo* sp. nicotinic AChR, or amino acids in its vicinity, may be elements of the APL binding site.[24] Such a location would also agree with the docking studies of Iorga et al.,[40] which propose the presence of an APL binding site on the inner funnel surface of the receptor, in the vicinity of K123. The mutagenesis study of Ludwig et al.[50] additionally suggests that mutation of F122 sensitively disrupts binding–response coupling, and that mutated K123 receptor exhibits modified responses to some agonists and to galanthamine. Furthermore, two different binding sites could explain the observed ligand

and nAChR subtype dependency,[16,50,60] as the sequences vary for all the different receptor subtype combinations, and thus the propagation mechanisms might be slightly different. Together, we interpret these data as an indicator of a second (inner) binding site for galanthamine from which the drug exerts its NCI activity. Conceivably, binding of galanthamine to this inner site locks the coupling hinge into a conformation that is detrimental to allosteric channel activation, and hence effects channel inactivation in a fashion similar to that of direct channel blockers. Consistent with this suggestion, this second binding site for galanthamine is of lower affinity relative to the outer site, it is photoaffinity labeled by physostigmine,[24] and it is not accessible for FK1 binding. Depending on the site of binding and the motion thereby induced, galanthamine may act as an enhancer (as APL), as is shown in Figure 9, or as an inhibitor (as NCI) on nAChR channel activity.

In summary, we can show that homology modeling in combination with molecular docking studies allows the identification and definition of putative APL binding sites on various nAChR subtypes. Computational studies have correctly guided experimental efforts toward the identification of functional relevant mutations of the receptor protein. Our results demonstrate the importance of feedback between theory and experiment for the validation of theoretical models and their use in further studies.

A more detailed and thorough investigation of the binding modes is the natural next step toward an understanding of the allosteric effect, and also to derive pharmacophores which could drive a rational drug design. The models could further be used to study the allosteric mechanism itself. This could lead to an understanding of the propagation of the APL binding effect to the ligand binding site or the gating of the channel itself. The latter remains a very challenging problem and is the focus of ongoing research.[37,61,62]

Experimental Section

Structure preparation

The multiple sequence alignment for the relevant sequences (Figure 1) used in this study was calculated with CLUSTAL-X[63] and visualized with TeXshade.[64] The alignment was manually refined to match the alignment of Le Novere et al.,[38] with sequence identities ranging from 20 to 50% between AChBP and the various receptor types. Based on this alignment, homology models for the extracellular part of the chicken and human $\alpha 7$ homopentameric receptors were calculated with SWISS-MODEL.[65] We also created a model representing the LBD of the human $\alpha 4\beta 2$ receptor. All structural models were subjected to WHATCHECK to identify possible problems in the structures (summary given in the Supporting Information). WHATCHECK identified only secondary packing problems for up to seven residues on a subunit. These problems indicate an unusual (relative to the known structures in the PDB) packing environment. Visual investigation of those residues showed none in the putative ligand binding sites.

As only the protein is used for model building, no information regarding crystallographic water was applied to any of the models or the docking process. The modeling procedure creates the side chain orientations based on a rotamer library[65] before a final energy-minimization step is performed. Localization of cavities was achieved by calculating the position of alpha spheres with the site finder as implemented in MOE.[52] All images were prepared with PyMOL (DeLano Scientific LLC, http://www.pymol.org).

Docking and clustering

All docking experiments were performed with FlexX,[66] specifying the complete receptor protein as the binding site and thus not limiting the search algorithm to certain regions of the protein. The well-accepted APLs galanthamine, codeine, physostigmine, and 5HT are used for ligand–protein docking. The docking algorithm treats the ligands as flexible, thus rotating single bonds unless they are in a ring. Various ring conformations were generated using the CORINA program.[67] As the tertiary nitrogen atoms in cyclic structures of the ligands investigated can potentially undergo inversion, we have always used both conformations with different pseudo-stereochemistry at the nitrogen atom of the ligands. In addition, we investigated various protonation states of the ligands, as the local pH of the binding sites is unknown. In this way, bias due to the initial conformation of the ligand is minimized.

All docked conformations, regardless of the ring conformation or the protonation state, were treated identically during clustering. Docking solutions found in the five similar binding sites in the homopentamers (or two binding sites in the case of the heteropentamer) were rotated in 3D space to overlay them in the reference frame of one dimer contact surface. These geometrical transformations and the clustering were performed by using tools from the CDK.[68] The all-atom RMSD between two conformations was used as the metric. For each ligand, the best scoring conformation was selected as the representative for the cluster. All conformations showing an RMSD ≤ 1 Å relative to the cluster representative are assigned to this cluster. The remaining unassigned structures were then iteratively processed in the same way until all structures were assigned to a cluster. All subsequent analyses were done with the cluster representatives.

Acknowledgements

E.L. thanks the Dr. Hilmer Foundation for the award of a doctoral scholarship and the FIZ Chemie, Berlin (Germany) for the "FIZ-Chemie-Berlin Award for Outstanding PhD Thesis 2004".

Keywords: acetylcholine receptor · APL · galanthamine · homology modeling · molecular modeling

[1] C. L. Masters, G. Simms, N. A. Weinman, G. Multhaup, B. L. Mcdonald, K. Beyreuther, *Proc. Natl. Acad. Sci. USA* **1985**, *82*, 4245–4249.
[2] J. Hardy, D. J. Selkoe, *Science* **2002**, *297*, 353–356.
[3] C. A. Davies, D. M. A. Mann, P. Q. Sumpter, P. O. Yates, *J. Neurol. Sci.* **1987**, *78*, 151–164.
[4] D. J. Selkoe, *Science* **2002**, *298*, 789–791.
[5] R. D. Terry, E. Masliah, D. P. Salmon, N. Butters, R. Deteresa, R. Hill, L. A. Hansen, R. Katzman, *Ann. Neurol.* **1991**, *30*, 572–580.
[6] A. L. Harvey, *Pharmacol. Ther.* **1995**, *68*, 113–128.
[7] M. Farlow, R. Anand, J. Messina, Jr., R. Hartman, J. Veach, *Eur. Neurol.* **2000**, *44*, 236–241.
[8] S. L. Rogers, L. T. Friedhoff, *Eur. Neuropsychopharmacol.* **1998**, *8*, 67–75.
[9] E. Giacobini, *Int. J. Geriatr. Psychiatry* **2003**, *18*, S1–S5.
[10] E. Giacobini, *Neurochem. Res.* **2003**, *28*, 515–522.
[11] E. F. R. Pereira, M. Alkondon, S. Reinhardt, A. Maelicke, X. Peng, J. Lindstrom, P. Whiting, E. X. Albuquerque, *J. Pharmacol. Exp. Ther.* **1994**, *270*, 768–778.

[12] A. Maelicke, A. Schrattenholz, M. Samochocki, M. Radina, E. X. Albuquerque, *Behav. Brain Res.* **2000**, *113*, 199–206.
[13] M. D. Santos, M. Alkondon, E. F. R. Pereira, Y. Aracava, H. M. Eisenberg, A. Maelicke, E. X. Albuquerque, *Mol. Pharmacol.* **2002**, *61*, 1222–1234.
[14] A. Maelicke, E. X. Albuquerque, *Eur. J. Pharmacol.* **2000**, *393*, 165–170.
[15] M. Samochocki, A. Höffle, A. Fehrenbacher, R. Jostock, J. Ludwig, C. Christner, M. Radina, M. Zerlin, C. Ullmer, E. F. R. Pereira, H. Lübbert, E. X. Albuquerque, A. Maelicke, *J. Pharmacol. Exp. Ther.* **2003**, *305*, 1024–1036.
[16] L. Texidó, E. Ros, M. Martín-Satué, S. López, J. Aleu, J. Marsal, C. Solsona, *Br. J. Pharmacol.* **2005**, *145*, 672–678.
[17] E. X. Albuquerque, M. D. Santos, M. Alkondon, E. F. R. Pereira, A. Maelicke, *Alzheimer Dis. Assoc. Disord.* **2001**, *15*, S19-S25.
[18] A. Maelicke, E. X. Albuquerque, *Drug Discovery Today* **1996**, *1*, 53–59.
[19] A. Maelicke, A. Schrattenholz, H. Schroder, *Sem. Neurosci.* **1995**, *7*, 103–114.
[20] A. Schrattenholz, E. F. R. Pereira, U. Roth, K. H. Weber, E. X. Albuquerque, A. Maelicke, *Mol. Pharmacol.* **1996**, *49*, 1–6.
[21] B. Schroeder, S. Reinhardt-Maelicke, A. Schrattenholz, K. E. McLane, A. Kretschmer, B. M. Conti-Tronconi, A. Maelicke, *J. Biol. Chem.* **1994**, *269*, 10407–10416.
[22] A. Storch, A. Schrattenholz, J. C. Cooper, E. M. Abdel Ghani, O. Gutbrod, K. H. Weber, S. Reinhardt, C. Lobron, B. Hermsen, V. Soskic, E. F. R. Pereira, E. X. Albuquerque, C. Methfessel, A. Maelicke, *Eur. J. Pharmacol.* **1995**, *290*, 207–219.
[23] J. Kuhlmann, K. O. Okonjo, A. Maelicke, *FEBS Lett.* **1991**, *279*, 216–218.
[24] A. Schrattenholz, J. Godovac-Zimmermann, H. J. Schafer, E. X. Albuquerque, A. Maelicke, *Eur. J. Biochem.* **1993**, *216*, 671–677.
[25] K. Brejc, W. J. van Dijk, R. V. Klaassen, M. Schuurmans, J. van Der Oost, A. B. Smit, T. K. Sixma, *Nature* **2001**, *411*, 269–276.
[26] S. B. Hansen, P. Taylor, *J. Mol. Biol.* **2007**, *369*, 895–901.
[27] Y. Bourne, T. T. Talley, S. B. Hansen, P. Taylor, P. Marchot, *EMBO J.* **2005**, *24*, 1512–1522.
[28] P. H. N. Celie, I. E. Kasheverov, D. Y. Mordvintsev, R. C. Hogg, P. van Nierop, R. van Elk, S. E. van Rossum-Fikkert, M. N. Zhmak, D. Bertrand, V. Tsetlin, T. K. Sixma, A. B. Smit, *Nat. Struct. Mol. Biol.* **2005**, *12*, 582–588.
[29] P. H. N. Celie, S. E. van Rossum-Fikkert, W. J. van Dijk, K. Brejc, A. B. Smit, T. K. Sixma, *Neuron* **2004**, *41*, 907–914.
[30] C. D. Dellisanti, Y. Yao, J. C. Stroud, Z.-Z. Wang, L. Chen, *Nat. Neurosci.* **2007**, *10*, 953–962.
[31] S. B. Hansen, G. Sulzenbacher, T. Huxford, P. Marchot, P. Taylor, Y. Bourne, *EMBO J.* **2005**, *24*, 3635–3646.
[32] R. J. Hilf, R. Dutzler, *Nature* **2008**, *452*, 375–379.
[33] A. B. Smit, N. I. Syed, D. Schaap, J. van Minnen, J. Klumperman, K. S. Kits, H. Lodder, R. C. van der Schors, R. van Elk, B. Sorgedrager, K. Brejc, T. K. Sixma, W. P. Geraerts, *Nature* **2001**, *411*, 261–268.
[34] N. Unwin, *J. Mol. Biol.* **1993**, *229*, 1101–1124.
[35] A. Miyazawa, Y. Fujiyoshi, M. Stowell, N. Unwin, *J. Mol. Biol.* **1999**, *288*, 765–786.
[36] N. Unwin, *J. Mol. Biol.* **2005**, *346*, 967–989.
[37] A. Miyazawa, Y. Fujiyoshi, N. Unwin, *Nature* **2003**, *423*, 949–955.
[38] N. Le Novere, T. Grutter, J. Changeux, *Proc. Natl. Acad. Sci. USA* **2002**, *99*, 3210–3215.
[39] V. Costa, A. Nistri, A. Cavalli, P. Carloni, *Br. J. Pharmacol.* **2003**, *140*, 921–931.
[40] B. Iorga, D. Herlem, E. Barre, C. Guillou, *J. Mol. Model.* **2006**, *12*, 366–372.
[41] T. Grutter, N. Le Novere, J. P. Changeux, *Curr. Top. Med. Chem.* **2004**, *4*, 645–650.
[42] A. B. Smit, P. H. Celie, R. Klaassen, P. van Nierop, S. E. van Rossum-Fikkert, W. J. van Dijk, R. van Elk, T. K. Sixma, *Nicotine Tob. Res.* **2005**, *7*, 658–658.
[43] R. H. Henchman, H.-L. Wang, S. M. Sine, P. Taylor, J. A. McCammon, *Biophys. J.* **2005**, *88*, 2564–2576.
[44] R. J. Law, R. H. Henchman, J. A. McCammon, *Proc. Natl. Acad. Sci. USA* **2005**, *102*, 6813–6818.
[45] Y. C. Xu, F. J. Barrantes, X. M. Luo, K. X. Chen, J. H. Shen, H. L. Jiang, *J. Am. Chem. Soc.* **2005**, *127*, 1291–1299.
[46] M. Schapira, R. Abagyan, M. Totrov, *BMC Struct. Biol.* **2002**, *2*, 1–9.
[47] S. M. Sine, *J. Neurobiol.* **2002**, *53*, 431–446.
[48] X. Huang, F. Zheng, C. G. Zhan, *J. Am. Chem. Soc.* **2008**, *130*, 16691–16696.
[49] K. Toshima, S. Kanaoka, A. Yamada, K. Tarumoto, M. Akamatsu, D. B. Sattelle, K. Matsuda, *Neuropharmacology* **2009**, 264–272.
[50] Details are described in: J. Ludwig, A. Höffle-Maas, M. Samochocki, E. Luttmann, G. Fels, A. Maelicke, unpublished results.
[51] H. R. Arias, *Neurochem. Int.* **2000**, *36*, 595–645.
[52] MOE, Chemical Computing Group (CCG), http://www.chemcomp.com (accessed August 13, 2009).
[53] H. Edelsbrunner, M. Facello, R. Fu, J. Liang, *Proceedings of the 28th Hawaii International Conference on System Sciences* **1995**, 256–264.
[54] E. F. R. Pereira, S. Reinhardt-Maelicke, A. Schrattenholz, A. Maelicke, E. X. Albuquerque, *J. Pharmacol. Exp. Ther.* **1993**, *265*, 1474–1491.
[55] M. Samochocki, M. Zerlin, R. Jostock, P. J. Groot-Kormelink, W. H. Luyten, E. X. Albuquerque, A. Maelicke, *Acta Neurol. Scand. Suppl.* **2000**, *176*, 68–73.
[56] G. M. Morris, D. S. Goodsell, R. S. Halliday, R. Huey, W. E. Hart, R. K. Belew, A. J. Olson, *J. Comput. Chem.* **1998**, *19*, 1639–1662.
[57] N. Mukhtasimova, C. Free, S. M. Sine, *J. Gen. Physiol.* **2005**, *126*, 23–39.
[58] M. Criado, J. Mulet, J. A. Bernal, S. Gerber, S. Sala, F. Sala, *Mol. Pharmacol.* **2005**, *68*, 1669–1677.
[59] G. Akk, J. H. Steinbach, *J. Neurosci.* **2005**, *25*, 1992–2001.
[60] C. J. G. M. Smulders, R. Zwart, I. Bermudez, R. G. D. M. van Kleef, P. J. Groot-Kormelink, H. P. M. Vijverberg, *Eur. J. Pharmacol.* **2005**, *509*, 97–108.
[61] S. M. Sine, A. G. Engel, *Nature* **2006**, *440*, 448–455.
[62] A. Mourot, T. Grutter, M. Goeldner, F. Kotzyba-Hibert, *ChemBioChem* **2006**, *7*, 570–583.
[63] J. D. Thompson, T. J. Gibson, F. Plewniak, F. Jeanmougin, D. G. Higgins, *Nucleic Acids Res.* **1997**, *25*, 4876–4882.
[64] E. Beitz, *Bioinformatics* **2000**, *16*, 135–139.
[65] T. Schwede, J. Kopp, N. Guex, M. C. Peitsch, *Nucleic Acids Res.* **2003**, *31*, 3381–3385.
[66] B. Kramer, M. Rarey, T. Lengauer, *Proteins* **1999**, *37*, 228–241.
[67] J. Sadowski, M. Wagener, J. Gasteiger, "CORINA: Automatic Generation of High-Quality 3D-Molecular Models for Application in QSAR" in: *QSAR and Molecular Modelling: Concepts, Computational Tools and Biological Applications* (Eds.: F. Sanz, J. Giraldo, F. Manaut), Prous Science Publishers, **1995**, pp. 646–651.
[68] C. Steinbeck, Y. Han, S. Kuhn, O. Horlacher, E. Luttmann, E. Willighagen, *J. Chem. Inf. Comput. Sci.* **2003**, *43*, 493–500.

Received: August 3, 2009
Published online on September 8, 2009

